

# Starting dynamics of a cw passively mode-locked picosecond Ti:sapphire/DDI laser

Nen-Wen Pu, Jia-Min Shieh, Yinchieh Lai, and Ci-Ling Pan

*Institute of Electro-optical Engineering, National Chiao Tung University, Hsinchu 300, Taiwan*

Received September 20, 1994

We show that, for a cw passively mode-locked picosecond Ti:sapphire/DDI laser, the first autocorrelation trace with negligible cw background occurs at a delay time of 20  $\mu\text{s}$ , or 1600 round trips from the first relaxation-oscillation peak. The trace suggests that the pulse consists of a primary pulse as short as 4.4 ps and of small secondary pulses that form a much wider pedestal of the trace, each containing  $\approx 50\%$  of the photon energy. Nearly transform-limited  $\approx 5$ -ps-wide Gaussian pulses were observed at a delay time of 40  $\mu\text{s}$ . After 45  $\mu\text{s}$ , the optical spectrum broadened considerably, and the time-bandwidth product increased to 4 in the steady state (after 60  $\mu\text{s}$ ).

The very early startup stage of mode locking is the key to the understanding of pulse formation in mode-locked lasers. Recently Sarukura and Ishida<sup>1</sup> and Kuo *et al.*<sup>2</sup> investigated the buildup dynamics of passively mode-locked Ti:sapphire lasers with HITCI (excited-state lifetime,  $\tau_{\text{ex}} \approx 1.2$  ns) and DDI ( $\tau_{\text{ex}} \approx 17$  ps) dye jets, respectively, as intracavity saturable absorbers. In these experiments the starting, or pulse-formation, time was estimated from the onset of second-harmonic signal<sup>1</sup> or extrapolation.<sup>2</sup> Detailed pictures of the initial pulse formation stage were not presented because of experimental difficulties. In this Letter we show, for the first time to our knowledge, how the laser evolves from cw to partial mode locking, and then to complete mode locking, by measuring the contrast ratio of transient autocorrelation traces, the second-harmonic generation (SHG) conversion efficiencies, and the transient optical spectra.

A block diagram of the experimental setup is shown in Fig. 1. The configuration of a picosecond passively mode-locked Ti:sapphire/DDI laser<sup>2</sup> is shown in the inset of Fig. 1. The lasing wavelength was set at  $\lambda = 770$  nm by a 0.5-mm-thick birefringent filter. Self-starting and sustaining of stable mode-locked pulses were obtained for DDI concentrations in the range of  $\approx 2 \times 10^{-5}$  to  $10^{-3}$  M. For the data presented below, the DDI concentration was  $3 \times 10^{-4}$  M. Pumped by an all-lines 6-W cw argon-ion laser, the Ti:sapphire laser routinely generates steady-state pulses with durations of  $\approx 5$  ps and an average power of 600 mW (5% output coupling) at  $\approx 79.4$  MHz. For the investigation of the dynamics of pulse formation in our laser, we employed an improved version of the time-gating technique<sup>2,3</sup> previously described. The cw argon-ion laser was mechanically chopped to produce 500-Hz square pulses with a FWHM of  $\approx 1000$   $\mu\text{s}$  and a rise time of 2  $\mu\text{s}$ . The output was divided into three beams. One of them was fed to a noncollinear autocorrelator or a monochromator and detected by a photomultiplier tube. The second beam was directly detected by a gated photomultiplier tube, gated by 1- $\mu\text{s}$  pulses delayed with respect

to the onset of the laser, and sent to a rf spectrum analyzer to monitor the transient beat notes. The third beam was detected by a fast photodetector for a real-time oscilloscope display of the pulse train. A boxcar integrator with a 50-ns gate then selected four pulses in a window at a given delay time and averaged the signal. By delaying the gate with respect to the chopped pumping signal, we can sample the transient temporal and spectral behavior of the output of the Ti:sapphire laser at consecutive moments in the evolution process.

From the real-time oscilloscope trace, we observed that the chopped laser output exhibited relaxation oscillation at 200 kHz during the first 15  $\mu\text{s}$  after the laser onset. Afterward, a pulse train appeared and soon became stable after an additional 30  $\mu\text{s}$ . Relaxation oscillation is caused by the interplay of population inversion and stimulated emission. Because gain saturation is not an important pulse-shaping mechanism in solid-state lasers, we do not expect relaxation oscillation to affect the starting dynamics of the Ti:sapphire/DDI laser.

The normalized background-free intensity autocorrelation traces as a function of the delay time are shown in Fig. 2, with the peak heights normalized to 2. Zero delay time coincides with the first relaxation-oscillation peak. The typical 2:1 contrast ratio<sup>4-8</sup> of a multimode randomly phased cw laser and 2:0 contrast ratio of a completely mode-locked laser, together with the intermediate cases of contrast ratios, were observed in the transient pulse-forming process. Curve (a) was measured at the onset of lasing, for which the relative phases of the modes were random. The corresponding normalized background-free autocorrelation trace had a baseline of unity and a coherent spike,<sup>6</sup> with a peak value of 2 and a FWHM width of  $\approx 9$  ps. Secondary spikes located at approximately a 10-ps delay from the coherent spike peak were due to the mutual correlation between side clusters of longitudinal modes observed in our transient spectral measurement (Fig. 3). The spectral width of these side clusters was  $\sim 0.2$  nm, and the clusters were separated by  $\sim 300$  GHz. We

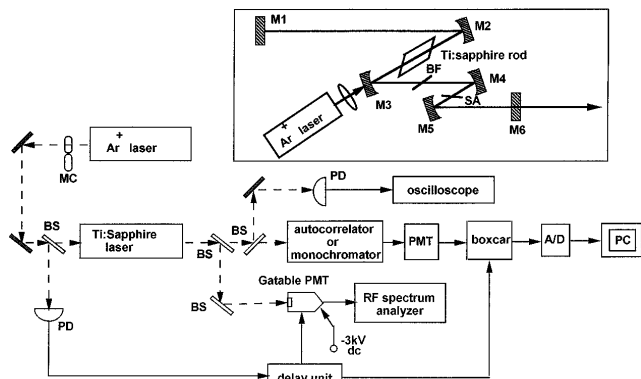


Fig. 1. Block diagram of the experimental arrangement: MC, mechanical chopper; BS's, beam splitters; PD's, photodetectors; PMT's, photomultiplier tubes; PC, personal computer; A/D, analog-to-digital converter. The inset shows the configuration of the passively mode-locked Ti:sapphire laser: SA, saturable absorber; BF, birefringent filter; M1–M6, mirrors.

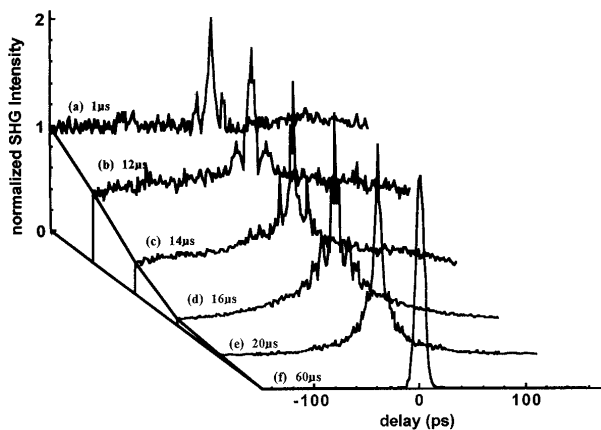


Fig. 2. Transient intensity autocorrelation traces at different delay times after the laser onset.

note that there was a spectral blue shift as the laser evolved to the steady state, as reported earlier.<sup>1,2</sup> This can be qualitatively explained: The absorption peak of DDI dissolved in ethylene glycol is at 710 nm, whereas the gain peak of Ti:sapphire is at 800 nm. As DDI became saturated during the evolution, the net gain of the laser shifted to the blue.

From curves (b) and (c) of Fig. 2, we can see an increase of the contrast ratio as the pulse began to form, but an apparent pulse profile has not yet appeared. At 16  $\mu$ s (1280 round trips), the autocorrelation trace displayed a low baseline, upon which was superposed a broad Lorentzian shoulder with a width  $\tau_G$  of  $\sim$ 155 ps, and a normalized height of  $\sim$ 0.3. The width of the central coherent spike remained unchanged throughout the buildup process up to this point. The width of the broad hill on which the spike rides,  $\tau_G$ , is proportional to the duration of the burst of light,<sup>4–10</sup> while the presence of a narrow central spike reveals the unclear appearance of the burst of light with numerous picosecond substructures<sup>5–7</sup> on it. At 20  $\mu$ s (1600 round trips), we observed the first autocorrelation trace with negligible cw background in the whole buildup process [curve (e) of Fig. 2]. The pedestal in the trace sug-

gests that the laser output is more like a short primary pulse with a number of much smaller secondary pulses.

Figure 4 shows the curve-fitting result of this trace [curve (e) of Fig. 2]. The central portion of the trace has a two-sided exponential profile. The corresponding primary pulse width is 4.4 ps. The shoulder of this trace (assumed to be Lorentzian) has a width of  $\sim$ 72 ps and a normalized height of  $\sim$ 0.23. Finally, the autocorrelation trace of the steady-state pulse is shown in curve (f) of Fig. 2. It suggests that the steady-state pulse shape is Gaussian, with a FWHM pulse width of 5 ps. We note that the pulse-evolution data coincide well with the transient optical spectra as well as with the beat-note spectra

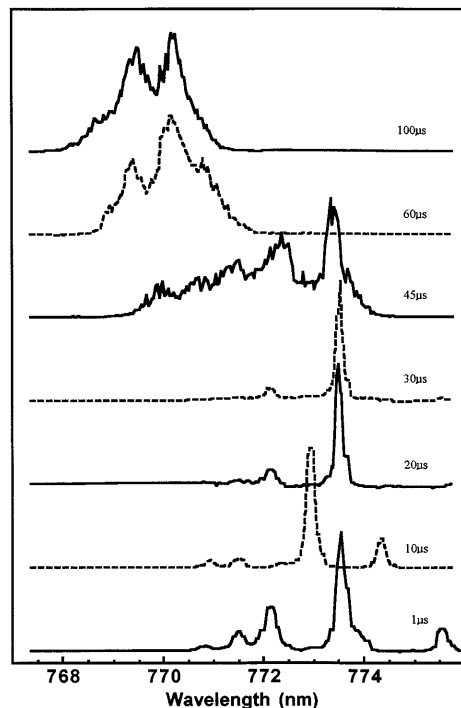


Fig. 3. Transient optical spectra of the output of the Ti:sapphire/DDI laser during the pulse buildup process.

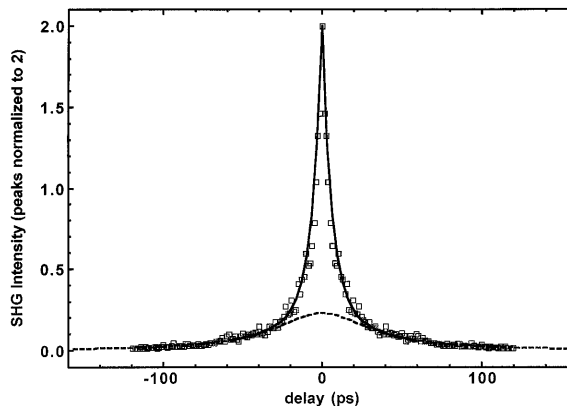


Fig. 4. Curve fitting of the autocorrelation trace at 20  $\mu$ s. The open squares are experimental data. The dashed curve is Lorentzian fit to the shoulder, with a pulse width of 72 ps. The solid curve is a symmetric two-sided exponential function superimposed upon the shoulder, with a pulse width of 4.4 ps.

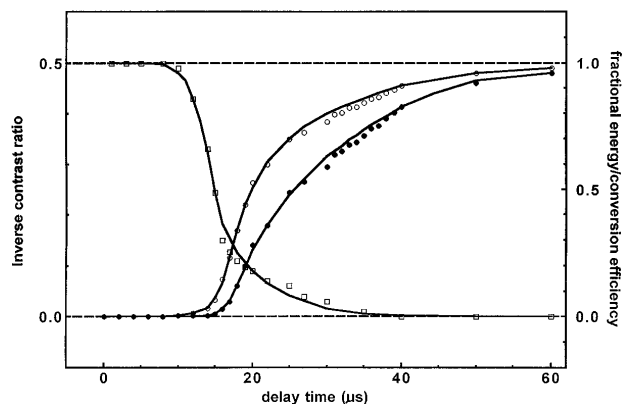


Fig. 5. Inverse contrast ratio  $R^{-1}$  (open squares), SHG conversion efficiency  $\epsilon^{(2)}$  (filled circles), and fractional energy  $\beta$  (open circles) as a function of the delay time.

(not shown). For the latter, we found that some beat notes began to emerge at  $16 \mu\text{s}$ . At  $30 \mu\text{s}$ , almost every beat note below 2 GHz has grown to a considerable extent. The steady-state low-frequency beat note spectrum (below 2 GHz) was observed beyond  $60 \mu\text{s}$ .

Although the autocorrelation trace fails to give the degree of mode locking, it has been pointed out by a number of workers<sup>5-11</sup> that the contrast ratio  $R$ , defined as the peak-to-shoulder ratio of the autocorrelation trace, i.e., the local contrast ratio,<sup>7</sup> would be a useful criterion for mode locking. In Fig. 5, we display the inverse contrast ratio,  $R^{-1}$ , as a function of time (open squares). This parameter shows apparent asymptotic behavior near the steady state, which is convenient for estimating the degree of mode locking. During the first  $10 \mu\text{s}$ , or the cw regime, the contrast ratio remained nearly a constant,  $R \approx 2$  or  $R^{-1} \approx 0.5$ . As the circulating energy inside the cavity increased and saturated the absorber dye, the output of the Ti:sapphire laser became modulated, and the value of  $R^{-1}$  began to decrease. When more longitudinal modes were locked with stronger phase interdependence, eventually a pulse with a background cw of nearly zero was formed at  $20 \mu\text{s}$ . The corresponding SHG correlation trace had a peak-to-shoulder contrast ratio of  $\approx 8.7$  ( $R^{-1} \approx 0.12$ ). Further locking of modal phases manifested itself as increasing  $R$  until the steady state, with practically infinite contrast ( $R^{-1} = 0$ ), was reached. At a delay of  $40 \mu\text{s}$ , a time-bandwidth product of  $\tau_p \Delta\nu \approx 0.5$  was measured. This is close to the transform limit of Gaussian pulses (0.44). After  $45 \mu\text{s}$ , the spectra (Fig. 3) broadened considerably, because of the effect of nonlinear self-phase modulation.<sup>12</sup> The time-bandwidth product eventually increased to  $\approx 4$ , much greater than the transform limit. This implies the existence of significant chirp within the pulse.

Also shown in Fig. 5 are the SHG conversion efficiency  $\epsilon^{(2)}$  (filled circles) and the fractional energy  $\beta$  (open circles) as a function of the delay time. The SHG conversion efficiency  $\epsilon^{(2)}$  is defined as  $E_1^{(2)}/E_2^{(2)}$ , where  $E_1^{(2)}$  denotes the actual SHG energy generated and  $E_2^{(2)}$  is the SHG energy that would have been generated by the fundamental wave of the same shape and of the same total energy but without

background. The fractional energy  $\beta$  is defined as  $E_p/E_{\text{total}}$ , where  $E_p$  is the energy of the pulse and  $E_{\text{total}}$  is the energy of pulse with background. We obtained the transient value of  $\epsilon^{(2)}$  by measuring the transient fundamental power, the SHG power, and the pulse width<sup>11</sup>:

$$\epsilon^{(2)} = \frac{\tau_p}{\tau_p^{\text{ss}}} \frac{(\overline{P}_\omega^{\text{ss}}/\overline{P}_\omega)}{(\overline{P}_{2\omega}^{\text{ss}}/\overline{P}_{2\omega})}, \quad (1)$$

where  $\tau_p$ ,  $\overline{P}_\omega$ , and  $\overline{P}_{2\omega}$  are transient pulse width, the fundamental power, and the SHG power, respectively. The parameters  $\tau_p^{\text{ss}}$ ,  $\overline{P}_\omega^{\text{ss}}$ , and  $\overline{P}_{2\omega}^{\text{ss}}$  are the corresponding steady-state values. It has been pointed out by Von der Linde<sup>10</sup> that  $\epsilon^{(2)}$  is insensitive to the pulse shape and is a very sensitive measure of the background level. In our experiment, at  $35 \mu\text{s}$ , for example, the inverse contrast ratio  $R^{-1}$  decreased by 99%, while the SHG conversion efficiency  $\epsilon^{(2)}$  grew to only  $\sim 70\%$ . The fractional energy,  $\beta$ , has an intermediate value of  $\sim 85\%$ . For the first autocorrelation trace with negligible background, at  $20 \mu\text{s}$ ,  $\beta \approx 50\%$ , i.e., approximately 50% of the photon energy, was in the primary pulse (see Fig. 4), whereas the remaining half was distributed among the small secondary pulses.

In summary, we have successfully measured, for the first time to our knowledge, the complete dynamic process of pulse formation from the start-up stage to the steady state in a picosecond passively mode-locked Ti:sapphire/DDI laser. Incomplete mode locking of various degrees, determined quantitatively from the inverse contrast ratio of the transient autocorrelation trace, the SHG conversion efficiency, and the fractional energy, are observed. These data are consistent with transient optical and beat-note spectral measurements.

This work was partially supported by the National Science Council of the Republic of China under grants NSC82-0417-E-009-397, -245, and -255.

## References

1. N. Sarukura and Y. Ishida, *Opt. Lett.* **17**, 61 (1992).
2. J.-C. Kuo, J.-M. Shieh, C.-D. Hwang, C.-S. Chang, and C.-L. Pan, *Opt. Lett.* **17**, 334 (1992).
3. J.-C. Kuo and C.-L. Pan, *Opt. Lett.* **15**, 1297 (1990).
4. P. W. Smith, M. A. Duguay, and E. P. Ippen, *Mode-Locking of Lasers* (Pergamon, Oxford, 1974).
5. D. J. Bradley and G. H. C. New, *Proc. IEEE* **62**, 313 (1974).
6. H. A. Pike and M. Hercher, *J. Appl. Phys.* **41**, 4562 (1970).
7. M. A. Duguay, J. W. Hansen, and S. L. Shapiro, *IEEE J. Quantum Electron.* **QE-6**, 725 (1970).
8. R. H. Picard and P. Schweitzer, *Phys. Rev. A* **1**, 1803 (1970).
9. H. E. Rowe and T. Li, *IEEE J. Quantum Electron.* **QE-6**, 49 (1970).
10. D. Von der Linde, *IEEE J. Quantum Electron.* **QE-8**, 328 (1972).
11. J. R. Klauder, M. A. Duguay, J. A. Giordmaine, and S. L. Shapiro, *Appl. Phys. Lett.* **13**, 174 (1968).
12. G. P. Agrawal, *Nonlinear Fiber Optics* (Academic, New York, 1989).